Journal of Asian Earth Sciences: X 3 (2020) 100024

Contents lists available at ScienceDirect

Journal of Asian Earth Sciences: X

journal homepage: www.journals.elsevier.com/journal-of-asian-earth-sciences-x

Evidence for Late Triassic crustal suturing of the Central and Southern Pamir

Dustin P. Villarreal[a,*], Alexander C. Robinson[a], Barbara Carrapa[b], James Worthington[b], James B. Chapman[c], Ilhomjon Oimahmadov[d], Mustafo Gadoev[d], Brian MacDonald[a]

[a] Department of Earth and Atmospheric Sciences, University of Houston, Houston, TX 77204, United States
[b] Department of Geosciences, University of Arizona, Tucson, AZ 85721, United States
[c] Department of Geology and Geophysics, University of Wyoming, Laramie, WY 82071, United States
[d] Institute of Geology, Earthquake Engineering and Seismology, Tajik Academy of Sciences, Dushanbe, Tajikistan

ARTICLE INFO

Keywords:
Pamir
Cimmerian
Gondwana
Tanymas
Paleotethys

ABSTRACT

The timing of closure of the Paleotethys and Rushan ocean basins and suturing of Gondwanan crustal fragments in the Pamir is not well resolved. Whereas the Central Pamir terrane is generally interpreted to have collided with the Northern Pamir terrane at the end of the Triassic, closure of the Rushan ocean and collision of the Southern Pamir terrane has been interpreted to be either broadly coeval (i.e., Late Triassic–Early Jurassic ~200 Ma) or have occurred significantly after closure of the Paleotethys in the Late Jurassic. New petrographic analyses and detrital zircon U-Pb data of the Lokzun Group Flysch and the terrigenous Darbasatash Group of the Southern Pamir terrane advocate for coeval terrane accretion of the Central and Southern Pamir terranes by the Latest Triassic. The Rhaetian Lokzun Group Flysch and the Early Jurassic Darbasatash Group have well-constrained stratigraphic ages and lie directly below and above a post-Cimmerian orogeny angular unconformity, respectively. Petrographic results for both successions indicate a recycled orogenic belt source, and detrital zircon age spectrum for both contain two prominent Phanerozoic age populations: an Early Silurian–Early Devonian (~440–408 Ma) and a Carboniferous Late Triassic (~350–222 Ma). These results suggest sediment was sourced from the Karakul-Mazar terrane, located in the northern Pamir, which requires closure of the Paleotethys and Rushan ocean basins and initial collision with the Central and Southern Pamir terranes by the end of the Late Triassic. Furthermore, these results suggest that the Northern Pamir terrane was topographically elevated relative to the surrounding terranes throughout the early Mesozoic.

1. Introduction

The Pamir lie at the western end of the Tibetan orogen and shares a broadly similar history of ocean basin closure, terrane accretion, and subsequent deformation as the Tibetan Plateau (Burtman and Molnar, 1993; Robinson, 2015; Yin and Harrison, 2000). Despite broad similarities, the timing of terrane accretion in the Pamir region remains less well constrained, raising questions of along-strike variability in the timing and nature of terrane accretion, correlation of geologic terranes across the orogen, and the nature of subsequent tectonic activity. One of the key outstanding questions in the Pamir is the timing of accretion of Gondwana terranes (Central and Southern Pamir terranes) to the Northern Pamir terrane, which closed the Paleotethys and Rushan ocean basins and resulted in the Pamir Cimmerian Orogeny. Although closure of the Paleotethys ocean and collision of the Central Pamir with the southern margin of Asia is generally interpreted to have occurred in the Latest Triassic (Angiolini et al., 2013; Burtman and Molnar, 1993; Robinson et al., 2004; Schwab et al., 2004), the timing of collision between the Southern Pamir and Central Pamir terranes is less clear and is suggested to have occurred either during the Late Jurassic to Early Cretaceous (He et al., 2018; Schwab et al., 2004) or during the Late Triassic to Early Jurassic (Angiolini et al., 2013). These disparate interpretations have significant implications for the correlation of terranes between the Pamir and Tibetan Plateau, and possible along-strike variations in the tectonic evolution of the Tibetan orogen. Here we address this debate through petrographic and detrital zircon provenance analysis of detrital sediments located above and below a regional unconformity developed after the Cimmerian Orogeny. Our results provide new insight into the timing of regional ocean basin closure and terrane accretion, as well as the nature of the Cimmerian orogeny in the Pamir.

* Corresponding author.
E-mail address: villarreal.dustin@gmail.com (D.P. Villarreal).

https://doi.org/10.1016/j.jaesx.2019.100024
Received 10 April 2019; Received in revised form 15 September 2019; Accepted 3 December 2019
Available online 14 December 2019

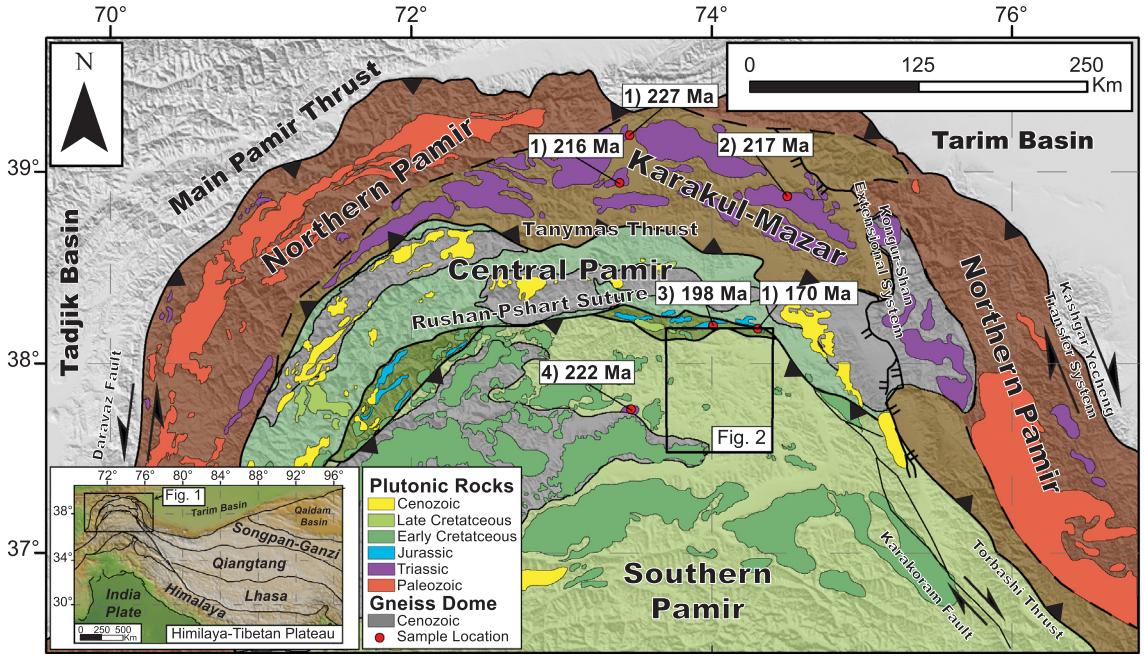

Fig. 1. Geologic map of the Pamir showing tectonic terranes, sutures, and the distribution of plutons and gneiss domes. Red circles represent sample locations and sources of data come from (1) Schwab et al. (2004); (2) Robinson et al. (2007); and (3) Chapman et al. (2017a,b); (4) Zanchetta et al. (2018) (modified from Schwab et al. (2004), Schmidt et al. (2011), Robinson (2015), Chapman et al. (2017a,b)).

2. Regional geology

The western portion of the Himalayan-Tibetan orogen consists of the Pamir-Karakoram mountain ranges. The Pamir mountains form a broad salient that has been displaced northward over the Tarim-Tajik basins along the north-vergent Main Pamir thrust system (MPT), which is kinematically linked with the left-lateral Darvaz Fault (DF) (Burtman and Molnar, 1993; Robinson, 2015) and right-lateral Kashgar Yecheng Transfer System (KYTS) (Cowgill, 2010; Sobel et al., 2011) to the west and east, respectively (Fig. 1). Northward displacement on the MPT has been suggested to be up to ~300 km as a result of the Cenozoic India-Asia collision (Burtman and Molnar, 1993), although several recent studies suggest significantly less Cenozoic displacement (Chapman et al., 2017a; Chen et al., 2018).

The Pamir-Karakoram salient has traditionally been divided into three tectonic terranes: The Northern Pamir, Central Pamir, and Southern Pamir-Karakoram, which are separated by the Tanymas and Rushan-Pshart thrust, respectively (Fig. 1). The Northern Pamir can be divided into two separate geologic terranes: (1) a northern portion which is the western continuation of the Paleozoic Kunlun terrane of Northern Tibet and (2) a southern portion, the Karakul-Mazar accretionary arc-complex, which is equivalent to the Triassic Hoh-Xil-Songpan-Ganzi terrane of Tibet (Schwab et al., 2004; Robinson et al., 2012). The Northern Pamir terranes were part of a cordilleran-style margin that developed along the southern margin of Asia through the late Paleozoic to Triassic during northward subduction of the Paleotethys oceanic lithosphere. Following closure of the Paleotethys ocean, Gondwana terranes of the Central and Southern Pamir were accreted to the southern margin of Asia, resulting in the Pamir Cimmerian orogeny (Burtman, 2010; Robinson, 2015; Schwab et al., 2004). In Tajikistan, this boundary separating Gondwanan crustal fragments from the Northern Pamir is defined by the northward-dipping Tanymas thrust (Burtman and Molnar, 1993) and in western China by the northward-dipping Torbashi thrust (Imrecke et al., 2019; Robinson et al., 2012).

The Central Pamir, Southern Pamir, and Karakoram terranes originated as part of the Gondwana supercontinent before separating in the late Carboniferous (Angiolini et al., 2015, 2013; Metcalfe, 2013). Evidence for rifting is recorded by clastic deposits that are directly overlain by Lower Permian deposits with cold water fauna. During rifting, the Rushan ocean basin opened between the Central and Southern Pamir during the Permian to Middle Triassic (Burtman, 2010; Leven, 1995), with possible rifting between the Southern Pamir and Karakoram terrane (Angiolini et al., 2013; Zanchi and Gaetani, 2011). After rifting, the Gondwana terranes drifted northward from their southern latitudes as the Paleotethys oceanic basin subducted below Asia. Conformably above the Lower Permian strata are Upper Permian clastic marine deposits that contain paleoequatorial fauna which are overlain by a regionally extensive Triassic carbonate platform in both the Southern Pamir and Karakoram terranes (Angiolini et al., 2013; Gaetani et al., 2013; Zanchi and Gaetani, 2011).

The Central Pamir, Southern Pamir, and Karakoram terranes have generally been interpreted to be the western equivalent of the Qiangtang terrane and part of the broad Cimmerian continent (Metcalfe, 2013). This correlation is based on similar histories of rifting and subsequent movement across the Paleotethys ocean that have been documented in the Qiangtang terrane (Dewey et al., 1988; Metcalfe, 2002), limited dextral-slip along the Karakoram fault (Phillips et al., 2004; Robinson, 2009; Searle and Phillips, 2007; Upadhyay et al., 2005), and stratigraphic similarities (Angiolini et al., 2013).

Timing of closure of the Paleotethys ocean and collision between the Central Pamir and Northern Pamir is interpreted to be Late Triassic in age, indicated by a cessation of igneous activity at the end of the Triassic in the Karakul-Mazar arc-complex and Early Jurassic zircon metamorphic ages from both sides of the Tanymas suture zone (Robinson, 2015; Robinson et al., 2012; Schwab et al., 2004; Xiao et al., 2002). However, timing of closure of the Rushan ocean and collision between the Central and Southern Pamir are less well constrained. Schwab et al. (2004) suggested that collision between the Southern Pamir and the Central Pamir was Late Triassic to Early Jurassic, based on the presence of Jurassic intrusive bodies in the Rushan-Pshart Zone (RPZ) and their interpretation that the Southern Pamir represents the western extent of the Lhasa terrane of Tibet. However, Angiolini et al. (2013) suggested that the timing of collision was Late Triassic to Early Jurassic in age due to petrographic analysis of a post-Cimmerian orogeny Early Jurassic terrigenous red bed from the Southern Pamir, along with limited displacement along the dextral Karakoram fault

(Phillips et al., 2004; Robinson et al., 2004; Searle and Phillips, 2007; Upadhyay et al., 2005). Further evidence for Late Triassic to Early Jurassic closure of the RPZ is the Triassic ophiolitic Bashgumbaz Complex (BSC) within the Southern Pamir which has been suggested to have been derived from the Rushan ocean basin (Pashkov and Shvol'man, 1979; Shvol'man, 1980, 1978). Recent work suggest that the BSC formed in a suprasubduction zone environment in the Late Triassic and was subsequently obducted onto the Southern Pamir during northward subduction of the Rushan ocean below the Central Pamir (Zanchetta et al., 2018).

The Southern Pamir and the Karakoram terrane are separated by the Wakhan-Tirich boundary Suture Zone (TBZ). Due to the lack of an ophiolite sequence or marine deposits, it is unclear whether an oceanic basin fully developed or whether it represents a region of attenuated continental crust (Zanchetta et al., 2018; Zanchi et al., 2000; Zanchi and Gaetani, 2011). Regardless of the nature of the boundary, the Karakoram was adjacent to the Southern Pamir by the Late Triassic to Early Jurassic (Zanchi and Gaetani, 2011).

3. Geology of the Southern Pamir

The Southern Pamir can be divided into a Southwestern (SW) and Southeastern (SE) Pamir that is separated by a Cenozoic extensional system (Schmidt et al., 2011; Schwab et al., 2004; Stübner et al., 2013). The SW Pamir is dominated by the Miocene Shakdhara gneiss dome which exposes mid- to lower-crustal rocks in the footwall of a regionally extensive detachment system (Schmidt et al., 2011; Stübner et al., 2013). The SE Pamir is composed of a dominantly Permian to Cretaceous sedimentary sequence that has experienced periodic contractional deformation from the Late Triassic to Late Cretaceous (Fig. 2) (Burtman and Molnar, 1993; Schwab et al., 2004; Angiolini et al., 2013; Robinson, 2015; Chapman et al., 2018).

Our field observations and geologic mapping within the Southeast Pamir are consistent with those documented by Angiolini et al. (2013, 2015) (Fig. 3). The lower portion of the sedimentary sequence consists of Permian through Triassic non-marine and marine sedimentary deposits, which Angiolini et al. (2013, 2015) classified as developing during a *syn*-rift to drift succession. The upper portions of this sequence consist of a Triassic carbonate platform (Korchagin, 2009, 2008) that is capped by the Lokzun group flysch deposit that is Rhaetian in age (Dronov et al., 2006). This Upper Paleozoic–Triassic sequence experienced very low grade metamorphism and significant deformation characterized by tight isoclinal folds, which are often overturned and heavily faulted, which is interpreted to have occurred during the Cimmerian Orogeny and closure of the Paleotethys and Rushan oceans (Angiolini et al., 2013). This sequence is capped by a regionally extensive angular unconformity (hereafter referred to as the post-Cimmerian unconformity).

Overlying the Late Paleozoic–Triassic, above the angular unconformity, is a Jurassic sequence. This sequence begins with the sparsely exposed Early Jurassic Darbasatash Group which is composed of shales, sandstones, and conglomerates. Conformably overlying the Darbasatash Group are the regionally extensive platform carbonates of the Gurumdi Group which are Hettangian in age (Dronov et al., 2006). The Jurassic sequence has experienced minor deformation interpreted to be Cretaceous in age consisting of broad open folds and local thrust faults (Chapman et al., 2018).

In this paper, we focus on the formations immediately below and above the post-Cimmerian unconformity, the Lukzon and Darbasatash groups respectively, addressing their provenance through petrographic and detrital zircon (DZ) analysis. These results yield critical constraints into the timing of ocean closure and terrane accretion within the Pamir.

4. Petrographic description

Petrographic analysis of detrital framework grains in sandstones has been shown to provide important insight into provenance type driven by tectonic processes (Dickinson and Suczek, 1979). For this study, petrographic thin sections were made for two samples from the Lokzun group and 4 samples from the Darbasatash Group. Four-hundred detrital framework grains (quartz, feldspar, and lithic rock fragments) were then counted for each sample following the Gazzi-Dickenson point counting method. Grain types identified are monocrystalline quartz (Qm), Feldspar (F), sedimentary (Ls) (excluding chert), chert (Lch), and metamorphic (Lm). For this study, feldspar lithic grains were not differentiated. Sedimentary lithic fragments consisted of siltstone, limestone, mudstone, and ooids. Chert lithic fragments (Lch) were separated into their own category due to their significance in convergent zones with most having undergone low grade metamorphism and recrystallization. Metamorphic lithic grains (Lm) consisted of polycrystalline quartz where there was the presence of grain boundary migration and grain suturing had occurred. The modal abundance was then calculated for each sample and plotted on the QmFLt Provenance Plot (Dickinson, 1985; Dickinson et al., 1983).

The Lokzun Group Flysch is the youngest Triassic strata and lies directedly below the post-Cimmerian unconformity (Fig. 3). The Lokzun Group has a well-developed slaty cleavage and experienced very low-grade metamorphism, slightly recrystallizing chert grains and precipitating authigenic quartz within depositional pore space. Petrographic analysis shows the two samples contain an abundance of monocrystalline quartz (65–74%), unaltered feldspar (< 5%), and lithic rock fragments (20–32%) (Fig. 4).

The Lower Jurassic Darbasatash Group is the oldest formation above the post-Cimmerian unconformity (Fig. 3). The sandstones from the Darbasatash Group contain an abundance of monocrystalline quartz (67–84%), feldspar (< 5%), and lithic rock fragments (15–30%). However, the feldspar in the Darbasatash Group has been heavily altered from diagenesis and, in many places, replaced by calcite (Fig. 4).

4.1. Results

Average sandstone framework compositions from the Lokzun Group and Darbasatash Group plot within the recycled orogen field on the QmFLt Provenance Plot (Dickinson, 1985) (Fig. 4). These results are consistent with previous analyses of the Jurassic Darbasatash group (Angiolini et al., 2013). However, although both samples share similarities in grain composition, grains in the Darbasatash Group are generally coarser than those in the Lukzon Group, indicating the Jurassic sandstones are not simply reworked Triassic flysch.

5. Detrital zircon analysis

5.1. Methods

Two slate samples from the Lokzun Group and five sandstone samples from the Darbasatash Group were processed for detrital zircons by conventional mineral separation methods of jaw crushing and disc milling, followed by water table and heavy liquid density separation, and final magnetic separation. Separated zircons grains were then mounted in epoxy and polished to expose the grain interiors. Zircon U-Th-Pb analyses were conducted via LA-ICP-MS at the University of Houston and at the University of Arizona Laserchon Center (laserchon.org). At the University of Houston, analyses were conducted using a Photon Machines Analyte.193 excimer laser attached to a Varian 810 Quadrupole mass spectrometer. Laser ablation consisted of a 25 μm spot and a fluence of 2.99 J/cm^2 at 10 Hz for 300 bursts resulting in an ablate time of ~30 s (proceeded with a background analysis of ~20 s). The data collected was then reduced using "U-Pb Reduction," an in-house software program written in MATLAB (Sundell, 2017). Laser ablation at the University of Arizona was performed with an ablate spot size of 20 μm using a Teledyne Photon Machines G2™ solid state NeF excimer system coupled to a Thermo Fisher Scientific ELEMENT 2™

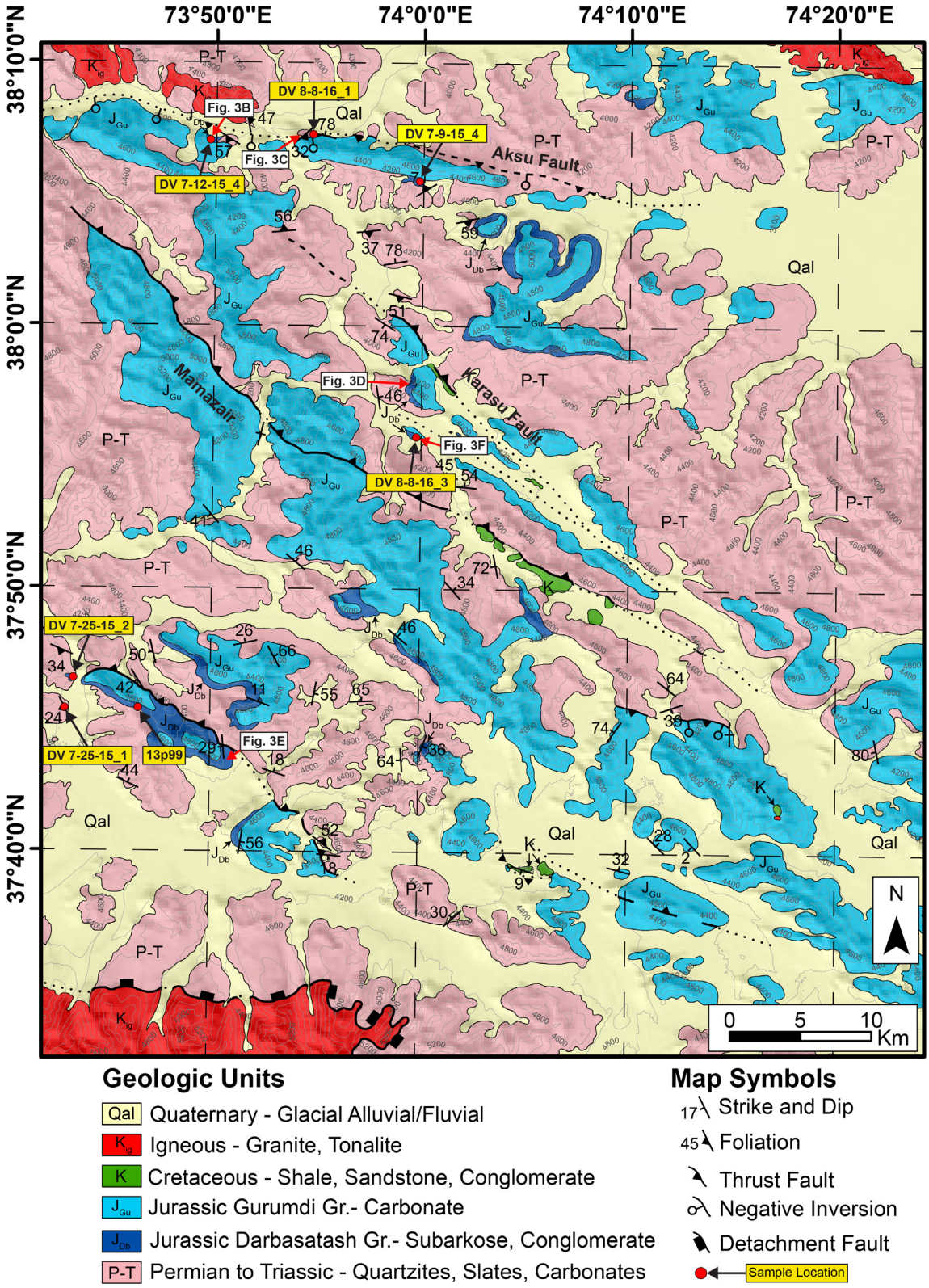

Fig. 2. Geologic field map of a portion of the eastern Southern Pamir terrane. Location of map is shown in Fig. 1. The Sample locations and detrital zircon data is presented in Data Repository 1 and 2. Location of field photos in Fig. 3 are labeled with red arrows indicating the direction in which the pictures were taken.

single collector inductively coupled plasma mass spectrometer (ICP-MS). Detailed information on data collection and reduction can be found in Gehrels et al. (2008). For each sample, 150–315 detrital zircons were analyzed and a minimum of 127 analyses were used to create individual probability diagrams using "isoplot" (Ludwig, 2003). Maximum depositional ages were calculated from the 3 youngest grains that overlapped within error and are within 2σ (Dickinson and Gehrels, 2009).

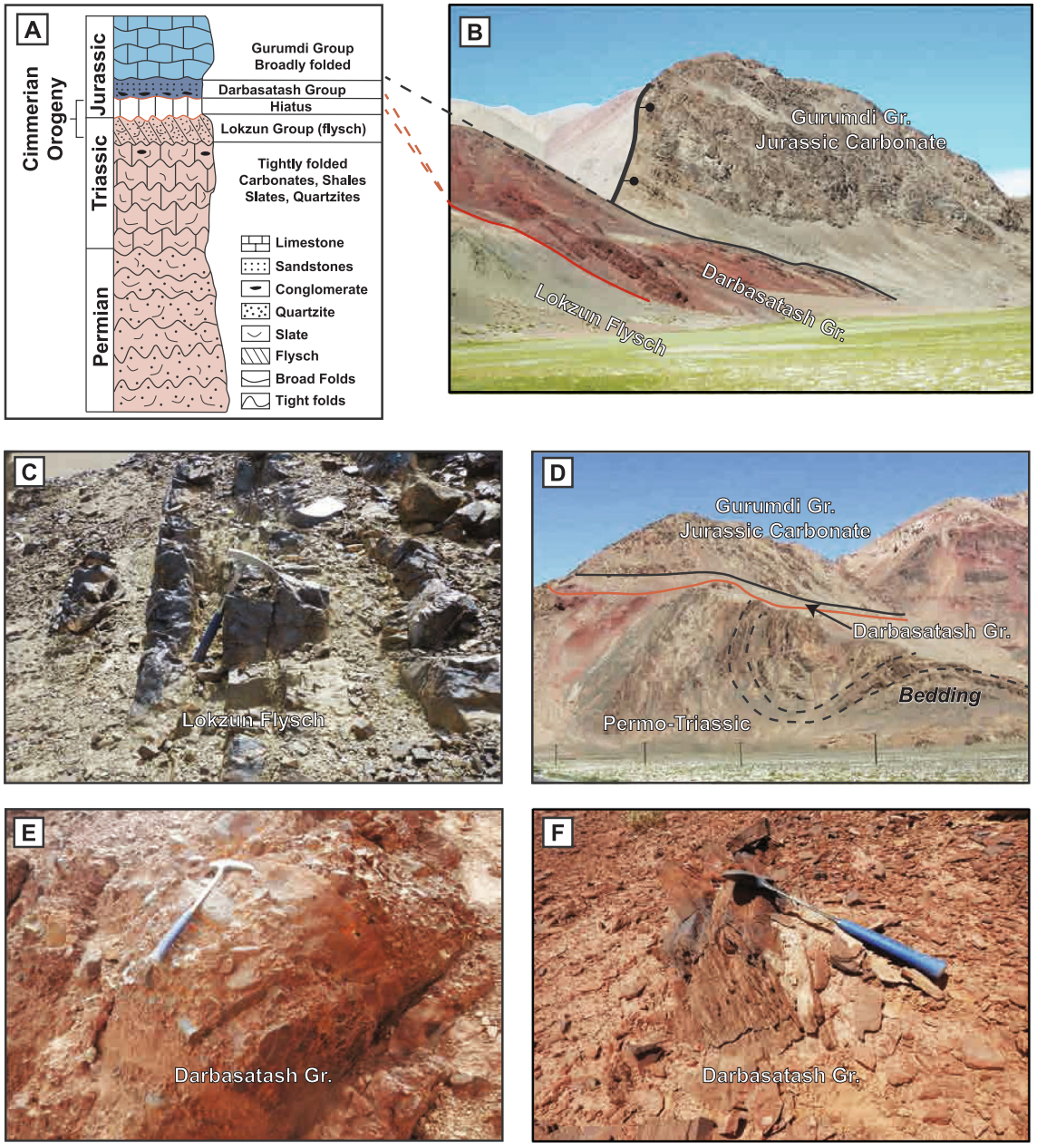

Fig. 3. (A) Simplified stratigraphic column of the Southeast Pamir showing prominent lithology and tightness of folded structures (modified from Angiolini et al., 2013). (B) Representative geology correlated to stratigraphic column in Fig. A (ridge location: 37.73N, 73.98E) (Landscape in the background is in the footwall of a small normal fault). (C) Lokzun Group Triassic flysch (location: 38.121N, 73.915N). (D) Post-Cimmerian unconformity (in red) separating the folded Permo-Triassic strata from the overlying sub-horizontal Darbasatash Group and Gurumdi Group (location: 37.95N, 74.00N). (E) Basal conglomerate of the Darbasatash Group (location: 37.732N, 73.845N). (F) Darbasatash Group sandstone (location: 37.929N 73.992E).

5.2. Triassic Lokzun group

5.2.1. Sample DV 8-08-16-1

Sample DV 8-08-16-1 is a slate from the footwall of the Aksu Thrust fault (Fig. 2).

200 zircon grains were analyzed with 183 being within 10 percent of error and having less than 25% discordance. The age distribution shows several key populations: two small Precambrian peaks and two prominent Phanerozoic peaks. The oldest Precambrian population is centered ~1858 Ma and the younger, broader population from ~1100 to 700 Ma. The older Phanerozoic population is Early Cambrian to Late Devonian with a peak at ~411 Ma. The youngest and most prominent population is middle Mississippian to Late Triassic (340–220 Ma) with two peaks at 303 and 264 Ma (Fig. 5). The youngest detrital zircon grain is 225 Ma, and the sample yields a maximum depositional age of 229 ± 9 Ma.

5.2.2. Sample DV 7-25-15-1

Sample DV 7-25-15-1 is a quartzite. 150 individual detrital zircon grains from the sample were analyzed with 125 having less than 10% error and having less than 25% discordance. The age distribution shows three minor Precambrian age populations and two prominent Phanerozoic populations. The Precambrian ages yield a small population between ~2600 and 2400 Ma, a medium population centered at ~1843 Ma (~2100–1600 Ma), and a small broad population between ~900 and 700 Ma. Phanerozoic ages yield an early Paleozoic population (~500–360 Ma) with a Silurian to Devonian peak and a younger and more prominent middle Mississippian to Late Triassic population

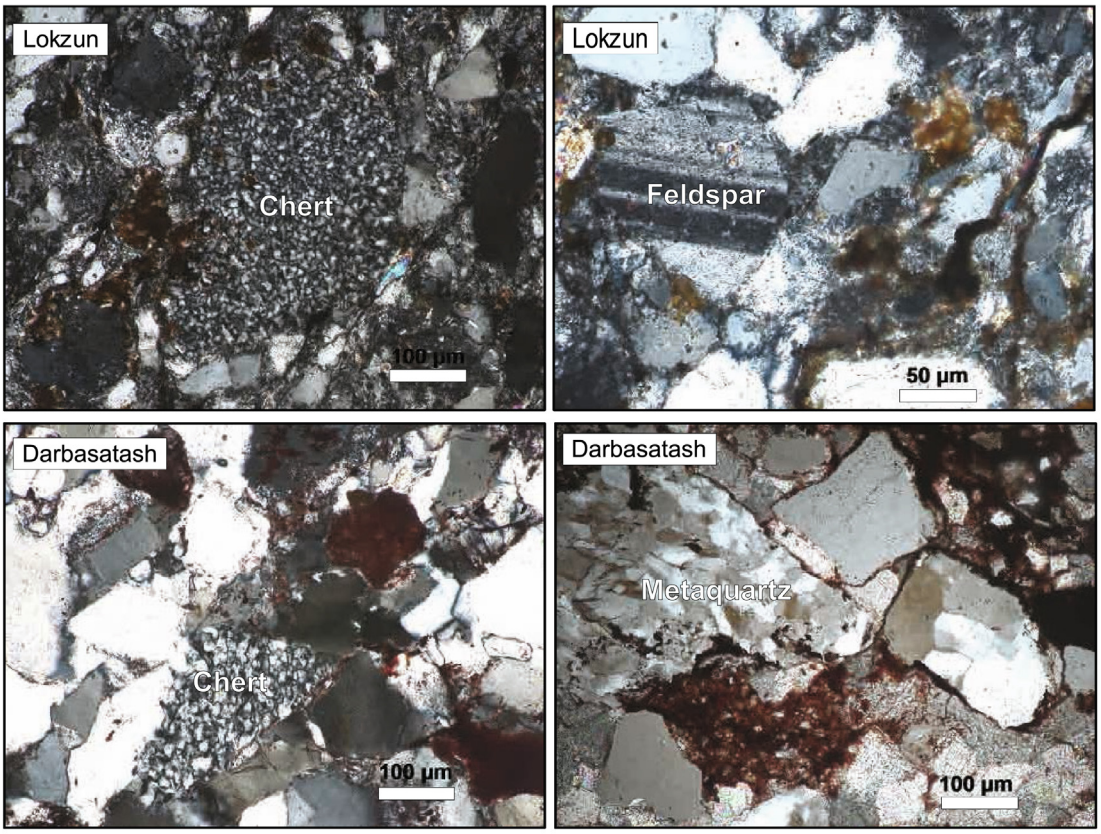

		Modal percentage								
Formation	Sample	Qm	F	Lt	Ls	Lch	Lm	Qm	F	Lt
Lokzun	DV 8-08-16_1	259	14	127	0	77	50	64.75	3.50	31.75
Lokzun	DV 7-25-15_1	304	15	81	0	55	26	76.00	3.75	20.25
Darbasatash	DV_7-9-15_4	303	23	74	0	14	60	75.75	5.75	18.50
Darbasatash	DV_7-12-15_4	337	5	57.6	0	32	26	84.33	1.25	14.41
Darbasatash	DV_8-08-16_3	302	3	95	46	18	31	75.50	0.75	23.75
Darbasatash	13P99	Not Counted						Not Counted		
Darbasatash	DV7-25-15_2	270	11	119	0	91	28	67.5	2.75	29.75

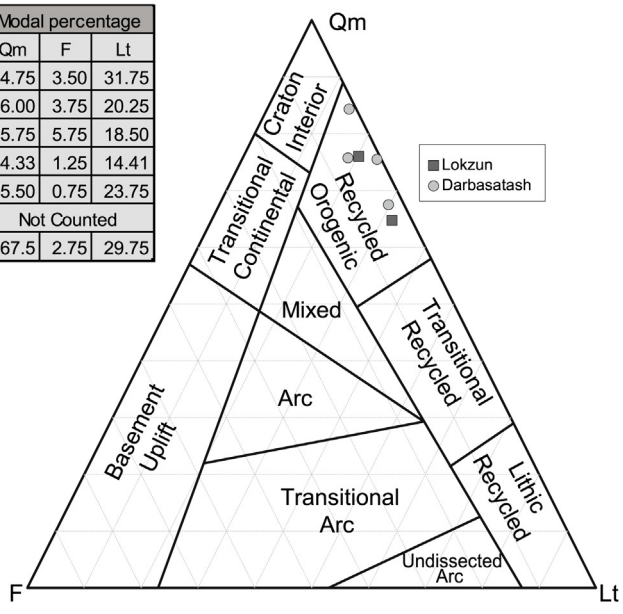

Fig. 4. Petrography of the Upper Triassic Lokzun Group flysch and Lower Jurassic Darbasatash Group terrigenous deposit. Lokzun Group and Darbasatash Group are dominated by monocrystalline quartz, minor chert, and polycrystalline quartz. Both contain rare feldspar; however, the feldspar is relatively unaltered in the Lokzun Group and heavily altered to replaced in the Darbasatash Group. 400 points were counted for each sample and modal percent was calculated and plotted on the QmFLt Provenance Plot (Dickinson, 1985). Qm = monocrystalline quartz; F = Feldspar; Lt = total lithics; Ls = sedimentary grains; Lch = chert grains; Lm = metamorphic grains.

(~340–200 Ma) with a prominent Triassic peak (~233 Ma) (Fig. 5). The youngest detrital zircon from the sample is 219 Ma and the sample yields a maximum deposition age of 227 ± 8 Ma.

5.3. Jurassic Darbasatash group

5.3.1. Sample DV 7-09-15-4

For sample DV 7-09-15-4, 200 individual grains were analyzed with 156 meeting requirements for plotting and interpretation. The age distribution shows one prominent Precambrian population at ~1858 Ma, with minor scattered ages between ~2600 and 2400 Ma

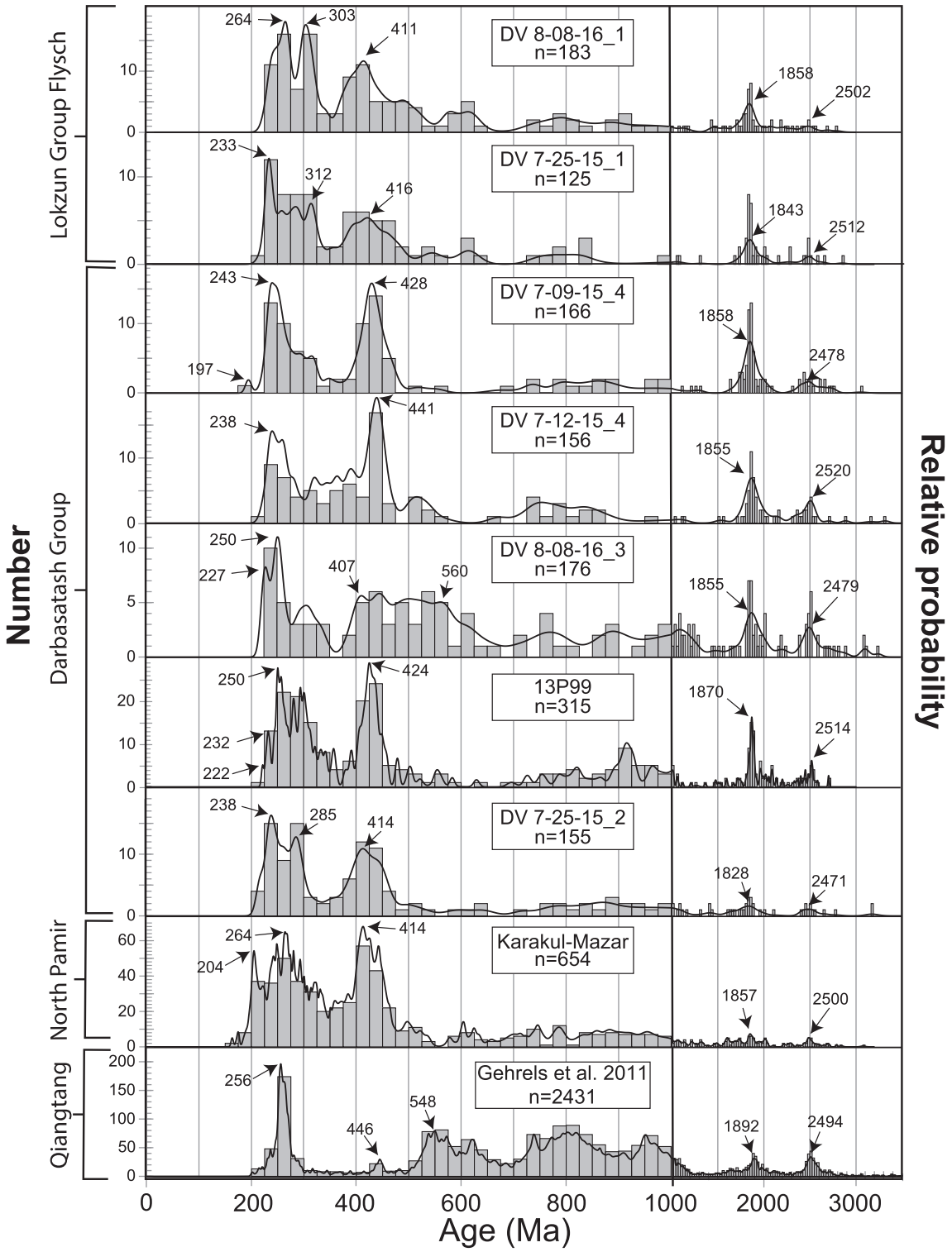

Fig. 5. Relative probability plots (black lines) and 25 Ma histograms (grey bars) for detrital zircon U-Pb geochronology from the Pamir and Qiangtang. Significant peaks are annotated by ages in Ma. The Lokzun Group flysch and Darbasatash Group are from this study and results are discussed herein. The Karakul Mazar is a cumulation of Robinson et al. (2012) and Imrecke et al. (2019). Qiangtang is a cumulation of the Northern and Southern Qiangtang from Gehrels et al. (2011).

and a small broad population between ~900 and 700 Ma. There are two prominent Phanerozoic populations: an early Paleozoic population with a strong Silurian peak at ~428 Ma and a Carboniferous to Late Triassic population (~340–220 Ma) with a strong Early Triassic peak (243 Ma) (Fig. 5). The youngest detrital zircon from the sample is an outlier at 195 Ma with the sample yielding a maximum deposition age of 229 ± 10 Ma.

5.3.2. Sample DV 7-12-15-4

For sample DV 7-12-15-4, 156 of the 200 individual zircon analyses met requirements for plotting and interpretation. The age distribution shows two prominent Precambrian peaks; a small one centered at ~2520 Ma (~2600–2400 Ma), a larger peak centered at ~1855 Ma (~2100–1600 Ma), as well as a small broad population between ~900 and 700 Ma. Phanerozoic ages yield a broad population of Paleozoic

through Triassic ages with two prominent peaks in the Silurian (~441 Ma) and Late Permian to Triassic (~238 Ma) (Fig. 5). The youngest age is 223 Ma and the sample yields a maximum deposition age is 230 ± 10 Ma.

5.3.3. Sample DV 8-08-16-3

For sample DV 8-08-16-3, 176 of the 200 detrital zircon analyses met requirements for plotting and interpretation. The age distribution yields two small Precambrian peaks and two prominent Phanerozoic peaks. The older Precambrian peak is ~2479 Ma (~2700–2400 Ma), with a younger more prominent peak at ~1855 Ma (~2100–1600 Ma), as well as a broad population from ~1300 to 700 Ma. The sample yields a broad prominent peak that is late Proterozoic–Devonian (~650–400 Ma) and a younger more prominent Permian to Triassic population (~270–220 Ma) (Fig. 5). The youngest detrital zircon grain is 225 Ma and the sample yields a maximum depositional age of 226 ± 8 Ma.

5.3.4. Sample 13P99

Sample 13P99 was analyzed at the University of Arizona Laserchon Center and possessed 315 ages meeting the previously-stated criteria. The age distribution for this sample has three minor Precambrian peaks and two prominent Phanerozoic peaks. The Precambrian peaks are at ~2514 Ma (~2600–2400 Ma), ~1870 Ma (~1900–1800 Ma) and have a broad distribution of ages from ~950 to 875 Ma. Phanerozoic ages yield two main populations: a strong Silurian through Early Devonian population and a Late Carboniferous to Late Triassic population (Fig. 5). The youngest detrital zircon grain is 221 Ma, and the sample yields a maximum depositional age is 225 ± 10 Ma.

5.3.5. Sample DV 7-25-15-2

For Sample DV 7-25-15-2, 155 of the 200 individual zircon analyses met requirements for plotting and interpretation. The age distribution shows three small Precambrian peaks and two prominent Phanerozoic peaks. The Precambrian peaks are a narrow population centered at ~2471 Ma (2600–2400 Ma), ~1828 Ma (2000–1600 Ma), and a broad population from ~1100 to 700 Ma. Phanerozoic ages yield a strong Early Ordovician to Late Devonian population and a strong bimodal Permian to Late Triassic population with peaks at ~285 and 238 Ma (Fig. 5). The youngest detrital zircon grain is 214 Ma and the sample yields a maximum depositional age of 216 ± 8 Ma.

5.4. Results

The Lokzun Group and Darbasatash samples from this study yield similar DZ age populations that have three minor Precambrian age groups and two prominent Phanerozoic age groups (Fig. 5). The two oldest Precambrian age populations of ~2600–2400 Ma and ~2000–1600 Ma are prominent in all samples analyzed, as well as being present in both Asian and Gondwanan terranes, and are not significant for the scope of this study. The youngest Precambrian age population in all samples is broad and generally ranges from ~1100 to 700 Ma. Although the Late Proterozoic age population is broad and varies between samples, there are no peaks statistically significant enough to affect comparison between the age distributions.

Phanerozoic detrital zircon ages for all seven samples are broadly similar, with all samples yielding two prominent age peaks: an Early Paleozoic peak that is generally Silurian to early Devonian (~440–410 Ma) and a younger peak that is generally Late Carboniferous to Triassic (320–200 Ma). We interpret this strong similarity to show that the samples were all sourced from the same terrane. One notable exception is sample DV 8-08-16_3 which has a broad late Neoproterozoic to Devonian age population (~560 Ma) (rather than the strong Silurian–Devonian population), although the sample has the same strong Carboniferous–Triassic population as the others. In comparing our results to previously-published detrital zircon populations from terranes in the Tibetan orogen, the two prominent Phanerozoic peaks are most similar to detrital ages from the Karakul Mazar Terrane of the Northern Pamir (Imrecke et al., 2019; Robinson et al., 2012) and Songpan-Ganzi terrane of northern Tibet (e.g. Ding et al., 2013; Weislogel et al., 2010, 2006). Further, the Phanerozoic populations are notably different than those obtained from the Gondwanan Qiangtang terrane of northern Tibet and Central Pamir (Gehrels et al., 2011; He et al., 2018). In particular, the strong Silurian–Devonian peak in most of the samples is absent in Gondwanan terranes, as are the strong Late Carboniferous to Triassic age populations (Fig. 5).

5.5. Statistical analysis

Literature reveals that previous quantitative comparison of DZ data sets has proven challenging, with various tests potentially yielding incorrect results (Saylor and Sundell, 2016; Vermeesch, 2005). In particular, the Kolmogorov-Simirnov (K-S) and Kuiper test p values have been shown to be problematic in comparing detrital zircon age populations. To address this concern, we conducted statistical comparisons between the samples using R^2 crossplot values calculated using Saylor and Sundell's (2016) DZstats. For a sample that has 50 age groups and n = ~150, an R^2 crossplot value greater than 0.70 ± 0.10 suggest the samples are related and have a common source. All but a few comparison values produced from quantitative analyses of the Lokzun Group, Darbasatash Group, and Karakul Mazar terrane fall within this range or are higher. R^2 crossplot values that lie below this range are associated with sample DV 8-08-16_3, which has a distinct late Proterozoic-early Paleozoic population, as discussed in the previous section (Data Repository Fig. 1). Although this statistical analysis supports our interpretation that the samples were all sourced from the same terrane, visual comparison of stacked probability diagrams may still be most reliable for this particular data set.

6. Discussion

Sediment provenance analyses of the Upper Triassic Lokzun Group and Lower Jurassic Darbasatash Group provide important new insights into the timing of suturing between the Southern and Central Pamir with the southern margin of Asia, the nature of the Cimmerian Orogeny in the Pamir, and the Mesozoic paleogeography of the Pamir.

6.1. Timing of suturing

Petrographic analyses of the Lokzun Group and Darbasatash Group samples show both formations are comprised of an abundance of monocrystalline quartz and lithic rock fragments (metamorphic quartz, chert, and siltstone) – typical of recycled orogenic deposits derived from continental convergence orogens, subduction zones, and foreland uplifts (Dickinson and Suczek, 1979). Furthermore, the formations plot in the recycled orogen field of the QmFLt Provenance Plot (Fig. 4) (Dickinson and Suczek, 1979), as has been shown previously for the Darbasatash group (Angiolini et al., 2013). Due to the nature of the contact between the Lokzun flysch and the Darbasatash (i.e., an angular unconformity), it is likely that the Darbasatash was partly sourced from the Lokzun Group. However, the monocrystalline quartz in the Darbasatash samples are slightly coarser than in the Lokzun Group, suggesting that the source of sediment for the formations was similar but that the Darbasatash was not primarily sourced from the Lokzun Group.

Based on the strong Late Carboniferous to Triassic signature, as well as the strong Silurian–Devonian population (Fig. 5) within our detrital zircon analyses, we interpret both the Lokzun Group and Darbasatash Group to have been largely sourced from the Karakul Mazar Terrane of the Northern Pamir. Furthermore, although Carboniferous through Triassic magmatism is well documented in the Northern Pamir and Western Kunlun Shan, the only Triassic magmatism documented in the Central and Southern Pamir is the Bashgumbaz Complex within the

Southern Pamir which has yielded an igneous age of ~220 Ma (Zanchetta et al., 2018) (Fig. 1). Although the Bashgumbaz Complex may be a partial source for Triassic ages, it does not account for the strong Permian–Triassic or Silurian–Devonian age populations present in the Lokzun Group or Darbasatash Group. Carboniferous–Triassic ages are also not present in detrital zircon results from pre-Jurassic sediments from Gondwanan terranes (Gehrels et al., 2011; Schwab et al., 2004; Robinson et al., 2007; Chapman et al., 2017a,b). Comparison of age populations from the Lokzun Group and the Darbasatash Group to Gondwanan Tibetan terranes suggest that the samples have limited local (i.e., Gondwanan) sources based on the lack of a strong late Proterozoic–Cambrian age population (Gehrels et al., 2011). As noted above, however, sample DV 8-08-16_3 appears to have had a more prominent local source due to a strong late Proterozoic to Early Devonian (~600–400 Ma) age population (Fig. 5).

Based on our evidence that both the Lokzun Flysch and Darbasatash formations were sourced from the Karakul-Mazar terrane, initial closure of both the Paleotethys and Rushan oceans must have occurred in the Late Triassic, with sediment from the Karakul-Mazar accretionary arc terrane being shed across the Central Pamir and onto the Southern Pamir immediately prior to deformation related to the Cimmerian orogeny (Fig. 6). Our results also suggest closure of the two oceans was broadly coeval. Initial collision between the southern margin of Asia and both the Central and Southern Pamir by the end of the Triassic is coeval with (or slightly pre-dates) closure of the Paleotethys ocean along the northern margin of the Qiangtang terrane to the east (Kapp and DeCelles, 2019 and references therein), clearly documenting that the Central Pamir and Southern Pamir were part of the larger Cimmerian terrane of Metcalfe (2013).

The timing of the Wakhan suture, which separates the Southern Pamir from the Karakoram, is not as well defined and may post-date the collision of the Southern Pamir and Central Pamir with the Northern Pamir. In the Karakoram deposition of the Aghil formation, carbonates continued through the Norian (later than Triassic carbonates in the Southern Pamir) and are then capped by the Lower Jurassic quartz-lithic sandstones of the Ashtigar Formation. Although the Ashtigar Formation has been suggested to be of similar age as the Darbasatash Group, its age is not well defined (Angiolini et al., 2013; Gaetani et al., 2013, 1993). Unlike the Gurumdi Group-Darbasatash Group angular unconformity, the Ashtigar Formation is conformable with the Aghil Formation. Instead, the Ashtigar Formation is unconformably overlain by the Lower Jurassic Yashkuk Formation, which has a Pliensbachian base (Gaetani et al., 2013, 1993) and is a molassic red sandstone that contains sedimentary and metasedimentary clasts. As the unconformity separating the Ashtigar and Yashkuk Formations is younger then the post-Cimmerian unconformity in the Southern Pamir, it suggests the collision of the Karakoram with the Southern Pamir occurred after accretion of the Central Pamir and Southern Pamir with the Northern

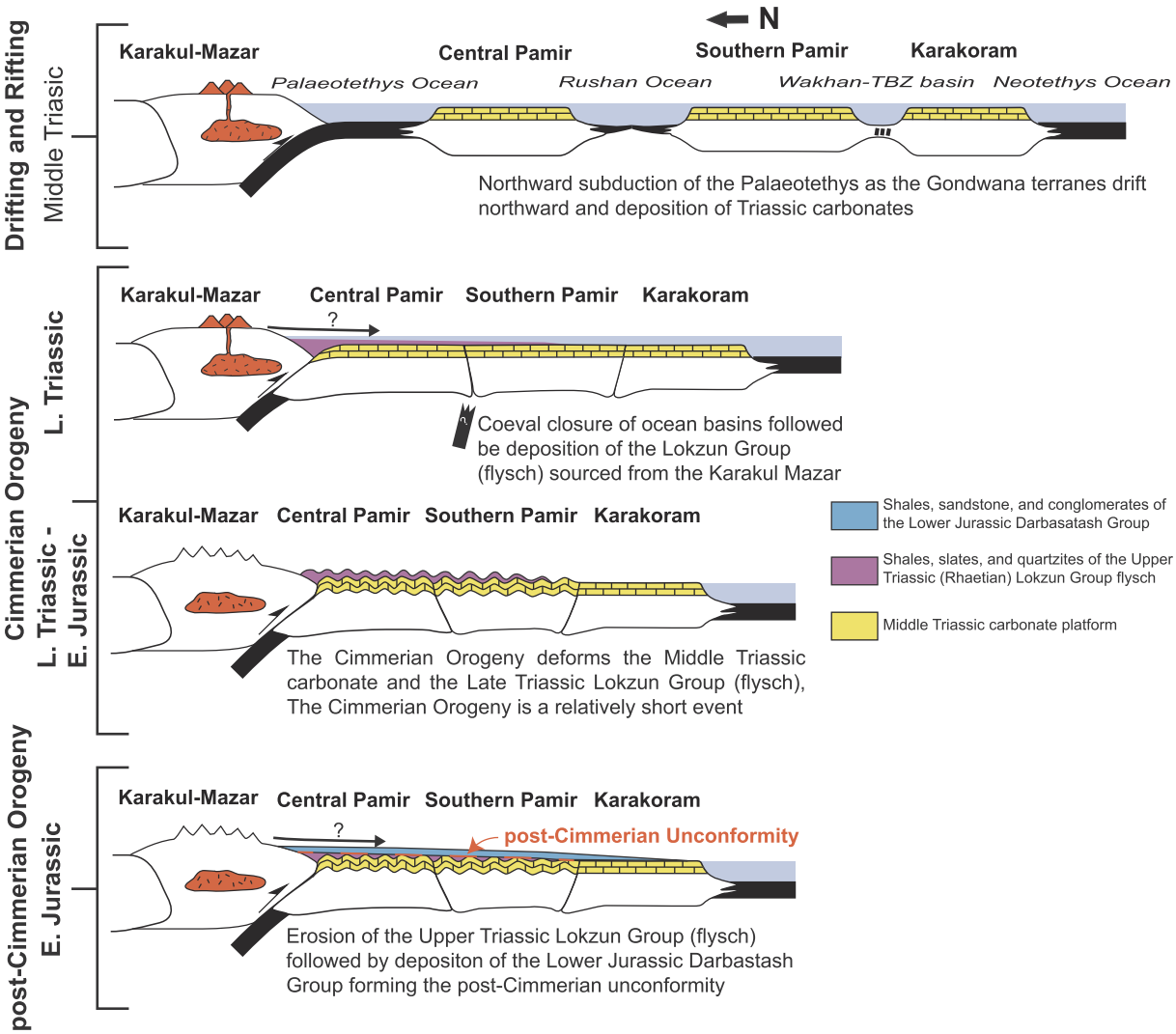

Fig. 6. Permian to Early Jurassic tectonic history of the Pamir showing rifting of the Gondwana terranes, implications of the Cimmerian Orogeny, and source and deposition of Late Triassic to Early Jurassic clastic rocks (modified from Angiolini et al. (2013) and Robinson (2015)).

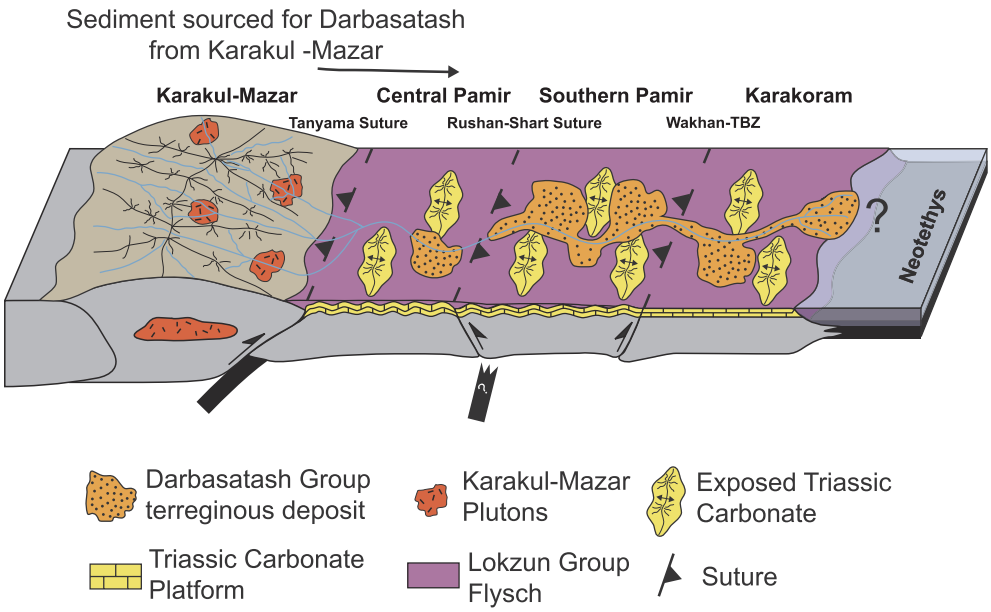

Fig. 7. Block model of the Pamir during the Early Jurassic. Note the Early Jurassic Darbasatash Group is sourced from the topographically elevated Karakul-Mazar Terrane and has a limited geographic exposure.

Pamir. Further studies of the Ashtigar and Yashkuk formations may shed new light onto possible sediment sources (e.g. from the Karakul-Mazar terrane, Rushan-Pshart Suture zone, or another source) and whether closure of the Paleotethys, Rushan Ocean, and Tirich Mir oceans were coeval or if closure of the Tirich Mir ocean occurred later (Fig. 6).

6.2. Implications for the Cimmerian Orogeny

Within the Pamir, the Cimmerian Orogeny is a regionally-developed deformation event that resulted from the accretion of the Central Pamir and Southern Pamir to the Paleozoic southern Margin of Asia. The Upper Triassic (Rhaetian) Lokzun Flysch, which records the initial collision of the Central and Southern Pamir with Asia, is the youngest formation deformed by the Cimmerian orogeny (Figs. 3 and 6). The regional unconformity that developed after Cimmerian deformation is overlain by the Lower Jurassic Darbasatash Group, the stratigraphic age of which is constrained by the overlying Hettangian age Gurumdi Group carbonate platform (Fig. 3) (Angiolini et al., 2013; Dronov et al., 2006). These constraints leave a narrow time period of several million years during which the Cimmerian Orogeny (and subsequent erosion) could have occurred, showing that the orogeny was a short-lived event within the Pamir. Further, both the very low grade of metamorphism of the rocks below the unconformity and the presence of a carbonate platform overlying the region immediately after indicate that crustal thickening related to the Cimmerian orogeny was limited, all of which indicate a “soft” collision between the Central and Southern Pamir and southern margin of Asia.

6.3. Implications for paleogeography

One of the interesting implications of the results of our study is that the Karakul-Mazar terrane of the Northern Pamir was a sediment source for clastic deposits in the Southern Pamir both before and after Cimmerian orogeny deformation. As the late Paleozoic–Triassic southern margin of Asia was a cordilleran-style margin prior to the Cimmerian Orogeny – with associated magmatism, crustal thickening, and high-grade metamorphism (Robinson et al., 2004; Schmidt et al., 2011; Schwab et al., 2004) – the Northern Pamir was likely a region of elevated topography (Fig. 6). More importantly, the Northern Pamir appears to have been a region of elevated topography relative to surrounding regions throughout the Mesozoic as (1) there are no post-Triassic sedimentary deposits in the Northern Pamir (and Western Kunlun), unlike the Tarim-Tajik basins and Central and Southern Pamir, (2) the Northern Pamir continued to be a source of sediment for the Tarim basin to the north throughout the Mesozoic and Cenozoic (Bershaw et al., 2012; Blayney et al., 2016; Cao et al., 2015; Sobel, 1999) as well as the Southern Pamir (i.e. the Darbasatash Group) in the Jurassic, and (3) cooling ages in the Northern Pamir record continued exhumation through the Jurassic and Cretaceous (Robinson et al., 2004). Finally, the discontinuous nature of exposures of the Darbasatash Group within the Southern Pamir support the interpretation that the Darbasatash Group filled paleo-lows and previously-incised valleys as suggested by Angiolini et al. (2013) (Fig. 7).

7. Conclusion

Our U-Pb detrital zircon and petrographic analyses from the Lokzun Group and Darbasatash Group, in combination with previous studies and geologic mapping of the Southeast Pamir, indicate the following:

1. Closure of the Paleotethys and Rushan Ocean was broadly coeval, with the Southern Pamir and Central Pamir accreting to the Northern Pamir (Paleozoic margin of Asia) by the end of the Triassic (Rhaetian) – resulting in the Cimmerian Orogeny.
2. The Karakul-Mazar detrital zircon signature is recorded in both the low-grade Upper Triassic (Rhaetian) Lokzun Group flysch, marking the timing of initial collision of the Central and Southern Pamir to the southern margin of Asia, and the post-Cimmerian Lower Jurassic Darbasatash Group that is overlain by the Hettangian age Gurumdi Group carbonate platform. This stratigraphic succession suggests that the Cimmerian orogeny was a short-lived event within the Pamir that resulted in minimal crustal thickening and that docking of the Gondwanan terranes was a “soft” collision.
3. Sourcing of both the Lukzon group and Darbasatash formation from the Karakul-Mazar terrane indicate that the Northern Pamir was topographically elevated relative to surrounding regions both prior to and after the accretion of the Central and Southern Pamir and may have represented a region of elevated topography throughout the Mesozoic.

4. Closure of the oceanic basins in the Pamir is coeval with the closure of the Paleotethys in Tibet, supporting interpretations that the Central Pamir and Southern Pamir are the western extension of the Qiangtang terrane of Tibet.

Declaration of Competing Interest

The authors declare that they have no known competing financial interests or personal relationships that could have appeared to influence the work reported in this paper.

Acknowledgments

This work was funded by National Science Foundation (NSF) grant EAR-1450899 and a Graduate Student Research Grant from the Geological Society of America to Villarreal. We thank Andrea Zanchi and an anonymous reviewer for constructive comments that helped improve the quality and clarity of this manuscript.

References

Angiolini, L., Zanchi, A., Zanchetta, S., Nicora, A., Vezzoli, G., 2013. The Cimmerian Geopuzzle: new data from South Pamir. Terra Nov. 25, 352–360. https://doi.org/10.1111/ter.12042.

Angiolini, L., Zanchi, A., Zanchetta, S., Nicora, A., Vuolo, I., Berra, F., Henderson, C., Malaspina, N., Rettori, R., Vachard, D., Vezzoli, G., 2015. From rift to drift in South Pamir (Tajikistan): Permian evolution of a Cimmerian terrane. J. Asian Earth Sci. 102, 146–169. https://doi.org/10.1016/j.jseaes.2014.08.001.

Bershaw, J., Garzione, C.N., Schoenbohm, L., Gehrels, G., Tao, L., 2012. Cenozoic evolution of the Pamir plateau based on stratigraphy, zircon provenance, and stable isotopes of foreland basin sediments at Oytag (Wuyitake) in the Tarim Basin (west China). J. Asian Earth Sci. 44, 136–148. https://doi.org/10.1016/j.jseaes.2011.04.020.

Blayney, T., Najman, Y., Dupont-Nivet, G., Carter, A., Millar, I., Garzanti, E., Sobel, E.R., Rittner, M., Andò, S., Guo, Z., Vezzoli, G., 2016. Indentation of the Pamirs with respect to the northern margin of Tibet: Constraints from the Tarim basin sedimentary record. Tectonics 35, 2345–2369. https://doi.org/10.1002/2016TC004222.

Burtman, V.S., 2010. Tien Shan, Pamir, and Tibet: history and geodynamics of phanerozoic oceanic basins. Geotectonics 44, 388–404. https://doi.org/10.1134/S001685211005002X.

Burtman, V.S., Molnar, P., 1993. Geological and geophysical evidence for deep subduction of continental crust beneath the pamir 281. doi: 10.1130/SPE281.

Cao, K., Wang, G.C., Bernet, M., van der Beek, P., Zhang, K.X., 2015. Exhumation history of the West Kunlun Mountains, northwestern Tibet: evidence for a long-lived, rejuvenated orogen. Earth Planet. Sci. Lett. 432, 391–403. https://doi.org/10.1016/j.epsl.2015.10.033.

Chapman, J.B., Carrapa, B., Ballato, P., DeCelles, P.G., Worthington, J., Oimahmadov, I., Gadoev, M., Ketcham, R., 2017a. Intracontinental subduction beneath the Pamir Mountains: constraints from thermokinematic modeling of shortening in the Tajik fold-and-thrust belt. Bull. Geol. Soc. Am. 129, 1450–1471. https://doi.org/10.1130/B31730.1.

Chapman, J.B., Robinson, A.C., Carrapa, B., Villarreal, D., Worthington, J., DeCelles, P.G., Kapp, P., Gadoev, M., Oimahmadaov, I., Gehrels, G., 2018. Cretaceous shortening and exhumation in the South Pamir terrane. Lithosphere. https://doi.org/10.1130/L691.1.

Chapman, J.B., Scoggin, S.H., Kapp, P., Carrapa, B., Ducea, M.N., Worthington, J., Oimahmadov, I., Gadoev, M., 2017b. Mesozoic to Cenozoic magmatic history of the Pamir. Earth Planet. Sci. Lett. 482, 181–192. https://doi.org/10.1016/j.epsl.2017.10.041.

Chen, X., Chen, H., Lin, X., Cheng, X., Yang, R., Ding, W., Gong, J., Wu, L., Zhang, F., Chen, S., Zhang, Y., Yan, J., 2018. Arcuate Pamir in the Paleogene? Insights from a review of stratigraphy and sedimentology of the basin fills in the foreland of NE Chinese Pamir, western Tarim Basin. Earth-Science Rev. 180, 1–16. https://doi.org/10.1016/j.earscirev.2018.03.003.

Cowgill, E., 2010. Cenozoic right-slip faulting along the eastern margin of the Pamir salient, northwestern China. Bull. Geol. Soc. Am. 122, 145–161. https://doi.org/10.1130/B26520.1.

Dewey, J.F., Shackleton, R.M., Chengfa, C., Yiyin, S., 1988. The tectonic evolution of the Tibetan Plateau. Philos. Trans. R. Soc. Lond. Ser. A, Math. Phys. Sci. 327, 379–413.

Dickinson, W.R., 1985. Interpreting provenance relations from detrital modes of sandstones. Proven. Arenites. https://doi.org/10.1007/978-94-017-2809-6_15.

Dickinson, W.R., Beard, L.S., Robert Brakenridge, G., Erjavec, J.L., Ferguson, R.C., Knepp, R.A., Alan, L.F., Ryberg, P.T., 1983. Provenance of North American Phanerozoic sandstones in relation to tectonic setting. Geol. Soc. Am. Bull. 94, 222–235. https://doi.org/10.1130/0016-7606(1983) 94<222:PONAPS>2.0.CO;2.

Dickinson, W.R., Gehrels, G.E., 2009. Use of U-Pb ages of detrital zircons to infer maximum depositional ages of strata: a test against a Colorado Plateau Mesozoic database. Earth Planet. Sci. Lett. 288, 115–125. https://doi.org/10.1016/j.epsl.2009.09.013.

Dickinson, W.R., Suczek, C.A., 1979. Plate-tectonics and sandstone compositions. Am. Assoc. Pet. Geol. Bull. 63, 2164–2182.

Ding, L., Yang, D., Cai, F.L., Pullen, A., Kapp, P., Gehrels, G.E., Zhang, L.Y., Zhang, Q.H., Lai, Q.Z., Yue, Y.H., Shi, R.D., 2013. Provenance analysis of the Mesozoic Hoh-Xil-Songpan-Ganzi turbidites in northern Tibet: implications for the tectonic evolution of the eastern Paleo-Tethys Ocean. Tectonics 32, 34–48. https://doi.org/10.1002/tect.20013.

Dronov, V.L., Melnikova, G.K., Salibjev, G.C., Bardashev, I.A., Minajiev, V.E., Muchabatov, N.M., 2006. Stratigraphic dictionary of the Pamir. Tech. Univ. Bergakademie Freib. 252.

Gaetani, M., Jadoul, F., Erba, E., Garzanti, E., 1993. Jurassic and Cretaceous Orogenic events in the North Karakoram: age constraints from sedimentary rocks. Himal. Tectonics Geol. Soc. Spec. Publ. 39–52.

Gaetani, M., Nicora, A., Henderson, C., Cirilli, S., Gale, L., Rettori, R., Vuolo, I., Atudorei, V., 2013. Refinements in the Upper Permian to Lower Jurassic stratigraphy of Karakorum, Pakistan. Facies. https://doi.org/10.1007/s10347-012-0346-9.

Gehrels, G., Kapp, P., Decelles, P., Pullen, A., Blakey, R., Weislogel, A., Ding, L., Guynn, J., Martin, A., McQuarrie, N., Yin, A., 2011. Detrital zircon geochronology of pre-Tertiary strata in the Tibetan-Himalayan orogen. Tectonics 30. https://doi.org/10.1029/2011TC002868.

Gehrels E., G., Valencia, V.A., Ruiz, J., 2008. Enhanced precision, accuracy, efficiency, and spatialresolution of U-Pb ages by laser ablation –multicollector –inductively coupled plasma –mass spectrometry. Geochem. Geophys. Geosyst. 9 (3). https://doi.org/10.1029/2007GC001805.

He, J., Kapp, P., Chapman, J.B., DeCelles, P.G., Carrapa, B., 2018. Structural setting and detrital zircon U-Pb geochronology of Triassic-Cenozoic strata in the eastern Central Pamir, Tajikistan. Geol. Soc. London, Spec. Publ. 483, SP483.11. https://doi.org/10.1144/SP483.11.

Imrecke, D.B., Robinson, A.C., Owen, L.A., Chen, J., Schoenbohm, L.M., Hedrick, K.A., Lapen, T.J., Li, W., Yuan, Z., 2019. Mesozoic evolution of the eastern Pamir. Lithosphere 11, 560–580. https://doi.org/10.1130/l1017.1.

Kapp, P., DeCelles, P.G., 2019. Mesozoic-Cenozoic geological evolution of the Himalayan-Tibetan orogen and working tectonic hypotheses. Am. J. Sci. 319, 159–254. https://doi.org/10.2475/03.2019.01.

Korchagin, O.A., 2009. Kaeveria fluegeli (Zaninetti, Altiner, Dager et Ducret, 1982) (Foraminifera) from Upper Triassic of the South-East Pamirs. Stratigr. Geol. Correl. 17, 62–67. https://doi.org/10.1134/S0869593809010055.

Korchagin, O.A., 2008. Foraminifers and stratigraphy of the Karatash Group (lower Triassic-Middle Anisian), the southeastern Pamir. Stratigr. Geol. Correl. https://doi.org/10.1134/S0869593808030027.

Leven, E.J., 1995. Permian and Triassic of the Rushan-Pshart zone (Pamir). Riv. Ital. di Paleontol. e Stratigr. 101, 3–16.

Ludwig, K.R., 2003. User's manual for Isoplot 3.00: a geochronological toolkit for Microsoft Excel. Berkeley Geochronol. Cent. Spec. Publ. 4, 70.

Metcalfe, I., 2013. Gondwana dispersion and Asian accretion: tectonic and palaeogeographic evolution of eastern Tethys. J. Asian Earth Sci. 66, 1–33. https://doi.org/10.1016/j.jseaes.2012.12.020.

Metcalfe, I., 2002. Permian tectonic framework and palaeogeography of SE Asia. J. Asian Earth Sci. 20, 551–566. https://doi.org/10.1016/S1367-9120(02)00022-6.

Pashkov, B.R., Shvol'man, V.A., 1979. Rift margins of tethys in the pamirs. Geotectonics 13, 447–456.

Phillips, R.J., Parrish, R.R., Searle, M.P., 2004. Age constraints on ductile deformation and long-term slip rates along the Karakoram fault zone, Ladakh. Earth Planet. Sci. Lett. https://doi.org/10.1016/j.epsl.2004.07.037.

Robinson, A.C., 2015. Mesozoic tectonics of the Gondwanan terranes of the Pamir plateau. J. Asian Earth Sci. 102, 170–179. https://doi.org/10.1016/j.jseaes.2014.09.012.

Robinson, A.C., 2009. Geologic offsets across the northern Karakorum fault: Implications for its role and terrane correlations in the western Himalayan-Tibetan orogen. Earth Planet. Sci. Lett. 279, 123–130. https://doi.org/10.1016/j.epsl.2008.12.039.

Robinson, A.C., Ducea, M., Lapen, T.J., 2012. Detrital zircon and isotopic constraints on the crustal architecture and tectonic evolution of the northeastern Pamir. Tectonics 31, 1–16. https://doi.org/10.1029/2011TC003013.

Robinson, A.C., Yin, A., Manning, C.E., Harrison, T.M., Zhang, S.H., Wang, X.F., 2007. Cenozoic evolution of the eastern Pamir: implications for strain-accommodation mechanisms at the western end of the Himalayan-Tibetan orogen. Bull. Geol. Soc. Am. 119, 882–896. https://doi.org/10.1130/B25981.1.

Robinson, A.C., Yin, A., Manning, C.E., Harrison, T.M., Zhang, S.H., Wang, X.F., 2004. Tectonic evolution of the northeastern Pamir: constraints from the northern portion of the Cenozoic Kongur Shan extensional system, western China. Bull. Geol. Soc. Am. 116, 953–973. https://doi.org/10.1130/B25375.1.

Saylor, J.E., Sundell, K.E., 2016. Quantifying comparison of large detrital geochronology data sets. Geosphere 12, 203–220. https://doi.org/10.1130/GES01237.1.

Schmidt, J., Hacker, B.R., Ratschbacher, L., Stübner, K., Stearns, M., Kylander-Clark, A., Cottle, J.M., Alexander, A., Webb, G., Gehrels, G., Minaev, V., 2011. Cenozoic deep crust in the Pamir. Earth Planet. Sci. Lett. https://doi.org/10.1016/j.epsl.2011.10.034.

Schwab, M., Ratschbacher, L., Siebel, W., McWilliams, M., Minaev, V., Lutkov, V., Chen, F., Stanek, K., Nelson, B., Frisch, W., Wooden, J.L., 2004. Assembly of the Pamirs: Age and origin of magmatic belts from the southern Tien Shan to the southern Pamirs and their relation to Tibet. Tectonics 23. https://doi.org/10.1029/2003TC001583.

Searle, M.P., Phillips, R.J., 2007. Relationships between right-lateral shear along the Karakoram fault and metamorphism, magmatism, exhumation and uplift: evidence from the K2-Gasherbrum-Pangong ranges, north Pakistan and Ladakh. J. Geol. Soc. London. 164, 439–450. https://doi.org/10.1144/0016-76492006-072.

Shvol'man, V.A., 1980. Mesozoic ophiolites in the Pamir. Geotectonics 14, 465–470.

Shvol'man, V.A., 1978. Relicts of the mesotethys in the pamirs. Himal. Geol. 8, 369–378.
Sobel, E.R., 1999. Basin analysis of the Jurassic–Lower Cretaceous southwest Tarim basin, northwest China. Geol. Soc. Am. Bull. 111, 709–724.
Sobel, E.R., Schoenbohm, L.M., Chen, J., Thiede, R., Stockli, D.F., Sudo, M., Strecker, M.R., 2011. Late Miocene-Pliocene deceleration of dextral slip between Pamir and Tarim: implications for Pamir orogenesis. Earth Planet. Sci. Lett. 304, 369–378. https://doi.org/10.1016/j.epsl.2011.02.012.
Stübner, K., Ratschbacher, L., Rutte, D., Stanek, K., Minaev, V., Wiesinger, M., Gloaguen, R., ProjectTIPAGEmembers, 2013. The Giant Shakhdara migmatitic gneiss dome, Pamir, India – Asia collision zone, I : Geometry and kinematics. Tectonics. https://doi.org/10.1002/tect.20057.
Sundell, K.E., 2017. Cenozoic surface uplift and basin formation in the Peruvian Central Andes. University of Houston.
Upadhyay, R., Rai, J., Sinha, A.K., 2005. New record of Bathonian-Callovian calcareous nannofossils in the eastern Karakoram block: a possible clue to understanding the dextral offset along the Karakoram Fault. Terra Nov. 17, 149–157. https://doi.org/10.1111/j.1365-3121.2005.00602.x.
Vermeesch, P., 2005. Statistical uncertainty associated with histograms in the earth sciences. J. Geophys. Res. Solid Earth 110, 1–15. https://doi.org/10.1029/2004JB003479.
Weislogel, A.L., Graham, S.a., Chang, E.Z., Wooden, J.L., Gehrels, G.E., Yang, H., 2006. Detrital zircon provenance of the Late Triassic Songpan-Ganzi complex: Sedimentary record of collision of the North and South China blocks. Geology 34, 97–100. https://doi.org/10.1130/G22944.1.
Weislogel, A.L., Graham, S.A., Chang, E.Z., Wooden, J.L., Gehrels, G.E., Survey, S.S.G., Analysis, M., 2010. Detrital zircon provenance from three turbidite depocenters of the Middle – Upper Triassic Songpan-Ganzi complex, central China : Record of collisional tectonics, erosional exhumation, and sediment production 2041–2062. doi: 10.1130/B26606.1.
Xiao, W.J., Windley, B.F., Chen, H.L., Zhang, G.C., Li, J.L., 2002. Carboniferous-Triassic subduction and accretion in the western Kunlun, China: implications for the collisional and accretionary tectonics of the northern Tibetan Plateau. Geology doi: 10.1130/0091-7613(2002)030 < 0295:CTSAAI > 2.0.CO;2.
Yin, A., Harrison, T.M., 2000. Geologic evolution of the Himilayan-Tibetan Orogen. Annu. Rev. Earth Planet. Sci. 28, 211–280. https://doi.org/10.1080/01947641003598252.
Zanchetta, S., Worthington, J., Angiolini, L., Leven, E.J., Villa, I.M., Zanchi, A., 2018. The Bashgumbaz Complex (Tajikistan): arc obduction in the Cimmerian orogeny of the Pamir. Gondwana Res. 57, 170–190. https://doi.org/10.1016/j.gr.2018.01.009.
Zanchi, A., Gaetani, M., 2011. The geology of the Karakoram range, Pakistan: The new 1:100,000 geological map of Central-Western Karakoram. Ital. J. Geosci. 130, 161–262. https://doi.org/10.3301/IJG.2011.09.
Zanchi, A., Poli, S., Fumagalli, P., Gaetani, M., 2000. Mantle exhumation along the Tirich Mir Fault Zone, NW Pakistan: pre-mid-Cretaceous accretion of the Karakoram terrane to the Asian margin. Geol. Soc. London, Spec. Publ. https://doi.org/10.1144/GSL.SP.2000.170.01.13.